CFD based Analysis on effect of Heat Transfer and Pressure Drop on Solar Air Heater

Synopsis Submitted in

Partial Fulfilment of the Requirements for the Degree of

Doctor of Philosophy

In

Mechanical Engineering

By

Rathod Hardikkumar Dhirajlal
Enrol. No.: 220810340005

Under the Supervision of

Dr. Dipak Dharmsibhai Patel
Provost, Dr. Subhash University - Junagadh

Dr. Siddharthsinh B. Jadeja [Co-Supervisor]
Research Assistant, University at Buffalo - USA

Dr. Subhash University
Dr. Subhash Road, Junagadh – 362001, Gujarat, India.

March 2026

DECLARATION

I, **Rathod Hardikkumar Dhirajlal**, Research scholar in the Department of Mechanical Engineering, declare that the work embodied in the Ph.D. thesis entitled, **"CFD based Analysis on effect of Heat transfer & Pressure Drop on Solar Air Heater"** is my original and bonafide work carried out by me under the supervision of **Dr. Dipak Dharmsibhai Patel**, Provost, Dr. Subhash University and the Co-supervision of **Dr. Siddharthsinh B. Jadeja**, Research Assistant, University at Buffalo - USA for a period from *August 2022* to *March 2026* at Dr. Subhash University.

I further declare that the contents embodied in this thesis have not been submitted for the award of any degree, diploma, associateship, fellowship or other similar title to any other University or Institute.

I confirm that I have duly acknowledged and given credit to the work of other researchers wherever cited in the text, tables, figures and the body of the thesis. I also declare that I have not will fully copied or reproduced others' work, data, results, etc., as reported in journals, books, magazines, reports, dissertations, theses, or available on websites, and claimed it as my own.

I shall be solely responsible for the **originality of the entire content** and any **plagiarism** found in the thesis.

Place:

Date: Signature of Research scholar:

Rathod Hardikkumar Dhirajlal

Enrol. No.: **220810340005**

CERTIFICATE

This is to certify that the thesis entitled **"CFD based Analysis on effect of Heat transfer & Pressure Drop on Solar Air Heater"** is a bonafide record of research work carried out by **Rathod Hardikkumar Dhirajlal** (Enrol. No. **220810340005**), Research Scholar, Department of Mechanical Engineering, School of Engineering & Technology, Dr. Subhash University - Junagadh, under our supervision during the period *August 2022 – March 2026*. To the best of our knowledge: (I) the candidate has not submitted the same research work to any other University or Institute for any Degree, Diploma, Associateship, Fellowship or other similar titles (II) the thesis submitted is a record of original research work done by the Research scholar during the period of study under our supervision, and (III) the thesis represents independent research work on the part of the Research scholar.

Place:

Date:

Name & Signature of Supervisor

Dr. Dipak Dharmsibhai Patel
Provost,
Dr. Subhash University – Junagadh.

Name & Signature of Co-supervisor

Dr. Siddharthsinh B. Jadeja
Research Assistant,
Department of Engineering Education,
University at Buffalo, USA

Index

Title		Page No.
TITLE		i
DECLARATION		ii
CERTIFICATE		iii
INDEX		iv
ABSTRACT		v
CHAPTER 1	INTRODUCTION	1
CHAPTER 2	LITERATURE REVIEW	4
	2.1. Overall Findings from Literature	8
	2.2. Research Gap	9
	2.3. Objectives	9
CHAPTER 3	COMPUTATIONAL ANALYSIS	10
	3.1. 3 Dimensional CFD Simulation	10
	3.1.1. Turbulence model Selection	13
	3.1.2. Governing equations	13
	3.1.3. Data reduction for CFD and experimental analysis	14
	3.1.4. Boundary condition	15
	3.1.5. Grid independence test	15
CHAPTER 4	EXPERIMENTAL STUDY	17
	4.1. Smooth absorber plate	18
CHAPTER 5	RESULTS AND DISCUSSION	20
	5.1. Effect on Nusselt number (Nu)	20
	5.2. Effect on Friction factor (f)	21
	5.3. Evaluation of Thermo hydraulic performance (THP)	22
	5.4. Comparison of Experimental and CFD result for Smooth plate	23
CHAPTER 6	CONCLUSIONS	25
	PUBLICATIONS	26
	REFERENCES	27

ABSTRACT

Solar air heaters (SAHs) are commonly used in applications where low to moderate temperature heat is required, such as heating of space, drying of agriculture crop and in many industrial heating processes. When smooth absorber plate is incorporated in SAH thermal efficiency remains low. This lower efficiency is because of viscous sub layer formed near the heating surface in the duct. It resists the air flow between the heating elements and airflow. By diffusing the artificial roughness over the heating surface is used as an active method to disrupt resisting viscous sub layer. This roughness creates turbulence in the air flow and the convective heat transfer in the SAH duct increases due to the well mixing of air.

In this research computational analysis as well as experimental study is done to calculate the thermo-hydraulic behaviour of the SAH. Single V+arc and Multiple V+arc shaped geometry is suggested for absorber plate. Computational Analysis is done using Ansys fluent 2024 R1 software. The turbulent flow is calculated by using SST k- ω turbulence model. Variation in Reynolds no. starting from 3000 to 11000 were maintained for velocity in air flow. In place of solar radiation uniform heat flow 1000w/m^2 was applied absorber plate for heating requirements. Geometrical and operating parameters like Height of rib is taken 2 mm, roughness pitch (P/e) – 10, duct aspect ratio (w/H) – 5, for both the roughness geometries and a rib attack angle of 60° in multiple V+arc geometry on absorber plate.

Combined V+arc geometry improves heat transfer rate. A considerable increase in Nusselt No. and Thermo-hydraulic performance parameter (THPP) when to smooth plate Friction factor also increases due to the provision of roughness element.

The results from experiments that are carried out in control condition also closely follows the trends from computational analysis. So it can conclude the reliability of the CFD method. The result also concludes improvement in heat transfer and pressure drop with the proposed geometry.

Chapter 1

Introduction

Today Morden society relies on the energy for the growth and smooth functioning. Due to the rise in population, increasing needs and continues technological development requires industrial growth, which increases global energy consumption. This increased demand of energy was fulfilled by the wood, coal, petroleum and natural gases for many years. But the amount of these resources are very limited in nature as well as its widespread use leads to many environment problems like air, water and soil pollution, climate change and global warming. So it is much needed to accept the use of sources which are sustainable and reusable in nature. Solar energy can be the most favourable replacement because of wide accessibility and sustainability.

Power generation, heating water or space, crops or seeds drying, industrial heating operations etc. can be achieved with the help of solar energy. It is used with the help of different technologies, in which the solar air heater is largely used and simple systems in recent years. The basic construction of it is shown in Figure 1.

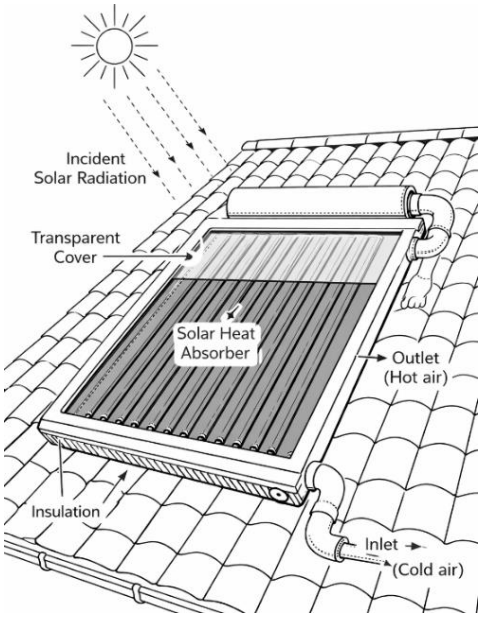

Figure 1.1: Solar Air Heater

Solar radiation is absorbed at the heating surface than it is conveyed to air that flowing through rectangular duct in SAH. This hot air can be used for various applications mentioned earlier. A

typical Solar Air heater has simple design, low working cost and minimum maintenance. So it is widely gaining attention to utilize the thermal energy consumption.

Besides its number of advantages its thermal efficiency is bit lower in conventional design. The main reason for this lower thermal performance is its low convective heat transfer coefficient. Heat carrying capacity and thermal conductivity of air is lower compared to liquids. A thin viscous sublayer grows in the airflow adjacent to heated plate.

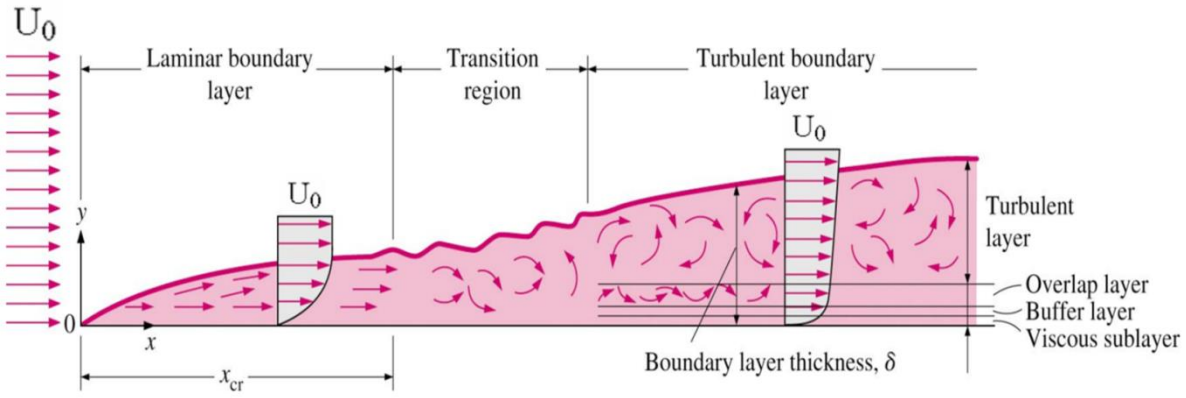

Figure 1.2: Velocity Distribution in Turbulent Flow Showing Viscous Sub layer Region [1]

The viscous sub layer shown in Figure 1.2 behaves like a thermal resistance in the path of heated absorber surface and air stream. This layer reduces the contact between the surface and airflow, which ultimately lowers rate of heat transfer. Therefore, the overall thermal effectiveness of any conventional SAH remains relatively low, so it makes their effective use restricted in larger heating applications.

To increase thermal effectiveness of SAH, various methods are developed by early researchers. From various methods one is method is to place the absorber plate with geometry of artificial roughness which is very effective to improve heat transfer. This roughness element disturbs the viscous sub layer which restricts the flow of air adjacent to heated plate. Turbulence and recirculation zones are formed in the airflow because of roughness element. This turbulence mixes the air which is very near to the heated surface which leads to improvement of heat transfer rate. When heat transfer increases the overall thermal hydraulic performance also increases.

The various studies are found focuses on development the artificial roughness geometry to develop thermal effectiveness of SAHs. Wire mesh, transverse ribs, inclined ribs, V shaped ribs, multiple V ribs, broken ribs, arc shaped ribs, protrusion ribs, dimple shaped rib are few

geometries which are incorporated on heated plate. To make these geometries effective parameters are studied like Rib pitch (p), Rib height (e), Relative Roughness Height (e/D), Relative Roughness Pitch (P/e), angle of attack (α) in V shaped ribs. These parameters affect the floe pattern of air in the SAH duct.

The flow behaviour is defined by the dimensionless parameter Reynolds no. (Re) which reveals turbulence in flow regime of SAH. The turbulent intensity increase with the rise in Reynolds no. also raises heat transfer rate.

Nusselt no. (Nu) and Friction factor (f) are key parameters to calculate the performance of SAH. The convective heat transfer from heating plate to flowing air is represented by Nusselt No. (Nu) and the resistance that the airflow faces due to the presence of roughness features are represented by Friction factor (f). So, it is necessary to carefully design the roughness element which increases the heat transfer but also keeps the low friction losses.

Due to increase in resistance in air flow because of artificial roughness pressure drop occurs. So to sustain the air flow it is necessary to pump more power. Therefore, to obtain better thermo-hydraulic performance, thorough adjustment of the operating conditions and the roughness design is required.

In this study, research is done to suggesting design of artificial roughness on absorber plate which improves the thermo-hydraulic performance parameter in comparison of smooth plate of SAH.

Chapter 2

Literature Review

It is well acknowledged that solar energy is a dependable and sustainable renewable energy source. Because of its straightforward design, little maintenance needs and eco-friendly functioning, solar air heaters (SAHs) are frequently utilized in a variety of applications. The three primary parts of a SAH are an absorber plate, insulation at the lowermost of the system and a transparent glass cover. After receiving solar radiation, the heating surface transmits the heat to air in duct. SAH with smooth plate however, have comparatively poor thermal performance. The advancement of viscous sub layer near heating plate and comparatively low heat conductivity of air are the primary causes of this restriction [2]. The viscous sub layer decreases heat transfer between heated plate and the moving air by acting as a thermal barrier.

A lot of research found on implementing roughness geometry on heated plate to increase thermal efficiency in SAHs. These roughness features increase heat transfer augmentation during the absorber plate and air by upsetting the laminar sub layer and encouraging localized turbulence in the airflow [4]. Nevertheless, the addition of roughness features also raises the duct's frictional resistance, which raises the pressure drop and increases the ratio of pumping power needed. To maximize the heat transfer improvement and minimize related friction losses, it is crucial to carefully design and optimize the roughness configuration [5].

When a fluid flows over a heated surface, a boundary layer is formed close to the wall. Within this region, a thin laminar sub layer develops, which restricts the heat transfer. Roughness on plate helps to disrupt this laminar sub layer and produces recirculation regions behind the roughness elements [6]. These vortices promote better mixing of air near heated wall which increase flow of heat. [5].

Sand-grain roughness in circular pipes was used in early experimental studies on turbulent flow over rough surfaces. These investigations suggest that roughness has impact on Reynolds no. friction factor and overall flow behaviour [7]. Three different areas of flow behaviour were found based on the experimental data.

1. Hydro dynamically smooth region – where roughness height has negligible effect.

2. Transitional roughness region – where friction factor depends on both Reynolds number and roughness height.

3. Fully rough turbulent region – where friction factor becomes independent of Re.

This studies shown that the reattachment of the separated shear layer behind roughness elements influences heat transfer enhancement. [8]

According to one study, roughness characteristics including relative pitch (p/e), relative roughness height (e/D), aspect ratio (W/H) and rib shape all affect heat transmission [9]. In order to assess heat transfer and pressure drop for various roughness configurations, statistical correlations were constructed. [10]

Thermal efficiency on behalf of Nusselt no., Friction Factor (f) and THPP are often used to evaluate the performance of SAH. The effectiveness of convective heat transmission between the absorber surface and the moving air is represented by the Nusselt number, which is directly correlated with the heat transmission. Artificial roughness increases airflow turbulence, which raises the temperature of the output air and raises the Nusselt number.

The friction factor represents pressure decrease due to roughness elements in the air duct. The studies shows the friction factor is estimated using the Darcy-Weisbach equation [8]. Although roughness elements improves heat transfer and also the friction factor (f). As a result, an ideal design must strike a compromise between pressure drop and improved heat transmission. THPP which takes into account both friction losses and improved heat transmission, was developed to examine overall performance [11]. When THPP is greater than unity a SAH with artificial roughness is considered thermally efficient. This condition indicates heat transfer enhancement achieved because of roughness is greater than the additional friction losses caused by them.

ASHRAE Standard 93–97 [3] standards are often followed for conducting controlled laboratory experiments on SAHs. Rectangular ducts with roughness element were used by several researchers to examine frictional properties and heat transmission of SAH. The rectangular duct is usually divided into three sections: an entering part, a test section, and an exit section. The test section's fully developed air flow is confirmed by the entry length, which is typically 5WH, and the departure length, which is 2.5WH. Electrical heaters are frequently used to replicate solar radiation with a constant heat flow of 1000 W/m^2. An orifice meter attached to a U-tube manometer is used to measure airflow through the duct, and a micro-manometer with a minimum

count of 0.001mm applied to monitor pressure drop. Calibrated thermocouples are positioned throughout heated plate and stream of air to detect temperature [12].

The experimental parameters commonly measured include:

- Solar irradiance
- Ambient temperature
- Air in and out Temperature
- Airflow rate
- Pressure drop

The ratio of rib height to the duct's hydraulic diameter is known as the relative roughness height (e/D). The interaction between roughness and sub layer that forms close to the heated surface is largely dependent on this parameter. According to earlier research, the effective roughness height is between 0.036 and 0.047, with an ideal value near 0.043 that improves the solar air heater's thermo-hydraulic performance [6][9].

If the rib height is lesser than the viscous sub layer thickness, the roughness has negligible effects heat transfer and if the rib height is too large, excessive turbulence is generated, resulting in higher pressure drop without progress in heat transfer.

Distance between successive roughness elements is determined by relative roughness pitch (p/e). To guarantee that the divided shear layer after the rib reattaches, proper pitch is required. According to studies, the ideal relative roughness pitch value is between 8 and 10. Heat transmission is reduced if the pitch ratio is less than 8 because the divided flow does not reattach to the surface. On the other hand, the impact of roughness becomes negligible if the pitch is too big [13].

Heat transfer enhancement is also influenced by the rib's angle of attack. The airflow is divided into major and secondary streams by inclined ribs, increasing turbulence and mixing in the flow field. When compared to transverse ribs, this enhances convective heat transmission. Because the air stays near the heated surface for a longer period of time, studies have shown that inclined rib configurations improve heat transmission [14].

The geometry and arrangement of ribs strongly affect turbulence intensity and flow pattern. Different rib geometries such as transverse ribs, V-shaped ribs, W-shaped ribs, dimples, grooves, and chamfered ribs have been investigated by several researchers. These roughness elements

create flow separation and reattachment zones that improves heat transfer with increase in friction losses.

Other researcher investigated inclined wire roughness for Re 3000 to 18000 and reported a 1.8 times rise in heat transfer with a 2.7 time rise of friction. [15] Studies show transverse wire roughness for Re range 5000 to 20000 and detected heat transfer enhancement factor ranging from 1.25 to 2.08 times [16]. Broken transverse ribs and reported heat transfer enhancement between 1.25 and 1.4 times, with thermal efficiency ranging from 51% to 83.5% [17]. Studies on metal mesh roughness showed 4 times rise in thermal heat transfer [18]. Similarly, wedge-shaped ribs showed a 2.4 Nusselt no. increase whereas friction factor rise 5.3 times [19]. At a 60° attack angle, tests on V-shaped ribs revealed a 2.30 times increment of Nusselt No. and 2.83 times friction factor. [20] In contrast, research on multi-V ribs found that Nu increased up to six times when compared to smooth ducts [21]. A maximum Nu increase of 6.74 times was recorded by one researcher using multi-V ribs with gaps [22].

Computational Fluid Dynamics (CFD) has been extensively employed in recent research to examine heat transmission and flow characteristics in solar air heaters. CFD allows visualization of velocity profiles, temperature distribution, and turbulence structures inside the duct. Most numerical investigations use turbulence models based on the Reynolds-Averaged Navier-Stokes (RANS) equations, such as: Standard k-ε model, Realizable k-ε model, RNG k-ε model, SST k-ω model

Among these models, the SST k-ω model has shown better capability for predicting separation and reattachment zones. Studies on circular transverse ribs using the RNG k-ε model and reported 2.31 times increase in Nu and friction factor increase up to 3.14 times compared to smooth ducts [23]. Broken ribs numerically reported 3.24 times increase in Nu and friction factor increase up to 3.85 times [24]. Research on rectangular ribs in triangular ducts found that at Reynolds number 15000, the friction factor increased up to 4.93 times and Nu increased by 2.07 times [25]. A maximum thermal efficiency of 72.41% in turbulators was reported by experimental and computational analysis on SAHs. [26].

2.1. Overall Findings from Literature

1. Artificial roughness introduced on the heated plate generates turbulence on the airflow which disturbs the viscous sub layer formed between the heated plate and air flow resulted in improved heat transfer rate.
2. Reynolds No. range adopted in most of the theoretical or experimental studies is from 2000 to 20000.
3. When Reynolds No. increases the Nussellt no. also increases, on other hand friction factor decreases when Reynolds No. increases.
4. Parameters like Rib pitch (p), Rib height (e), relative roughness height (e/D), relative roughness pitch (P/e), aspect ratio (W/H), angle of attack (α) impacts the performance of the SAH.
5. Relative roughness height (e/D) ideally remains in between 0.036 to 0.047, 0.043 is most suitable value to enhance the thermo-hydraulic performance.
6. Flow reattachment increases due to the relative roughness pitch (P/e). When the p/e ratio is between 8 and 10, the divided shear layer may effectively reconnect and enhance heat transfer.
7. Air flow patterns in the duct are influenced by the angle of attack of the ribs, 60^0 rib angle can increase the turbulence and strong secondary flow.
8. Nusselt No. rise recorded in the range of 1.8 to 6.74 compared to smooth absorber plate in experimental studies.
9. In artificial roughened ducts Friction factor rise recorded in the range of 2 to 6 times compared to ducts with smooth absorber plate due to turbulence and flow opposition.
10. Thermo-hydraulic performance parameters (THPP) rise recorded in the range of 3.4 to 3.7 when the V shaped and arc shaped roughness elements are incorporated on absorber plate.
11. When the experimental studies are compared with the computational analysis, turbulence models like RNG k-ε and SST k- ω are in good agreement. CFD Computational fluid dynamics studies can be used to simulate the behaviour of air, recirculation zones, heat transfer improvements and descent in pressure.

2.2 Research Gap

1. V shaped ribs delivers better secondary flow whereas arc shaped ribs improves the THPP with low friction losses, when other roughness geometries are compared.
2. Major researchers have adopted the single roughness geometries on heating plate, very few examinations are found with combined or hybrid rib geometries.
3. The combination of V-shaped and arc-shaped roughness geometry in SAHs have not well studied analytically or numerically. So, it needs to be well studied to achieve the better THPP in SAHs.

2.3 Objectives

1. To analyse the enactment of Solar Air Heater, used for low to moderate temperature, having combination of V+Arc shaped roughness geometry using CFD software.
2. To fabricate the experimental set-up in order to perform the experiments under the same conditions used in simulation.
3. To compare the Experimental and Computational results.

Chapter 3

Computational Analysis

A numerical technique called computational fluid dynamics (CFD) makes use of computer simulations to study fluid flow, heat transport, and related physical properties. It is currently an essential tool in many technical and industrial applications. In this work, CFD is used to check the flow pattern and heat transfer within a solar air heater in order to identify a configuration that can improve the heater's overall performance.

The distribution of temperature and pressure along the absorber surface as well as the airflow behaviour inside the duct are examined by CFD study of the V+arc roughness geometry absorber plate. The numerical study of roughened SAH duct is carried out by using the ANSYS fluent R1 software to solve conservation of mass, momentum and energy equations.

Some of the assumptions are made during the numerical analysis:

1. The airflow inside the duct is assumed steady and fully turbulent.
2. The duct walls, absorber plate, and roughness elements are considered homogeneous and isotropic.
3. The walls are subject to a no-slip boundary condition, and it is assumed that the fluctuation in air density is minimal.
4. Radiative heat transfer inside the duct is neglected during the analysis.

3.1. 3 Dimensional CFD Simulation

A rectangular SAH duct with three sections—entrance, test, and exit—is the 3D computational domain taken into consideration in this work showed by figure 3.1. In order to replicate solar heating, a constant heat flux boundary condition is introduced to the aluminum absorber plate of length L2, which is located in the test section. The test portion is situated upstream of the entry section (L_1) and downstream of the exit section (L_3).

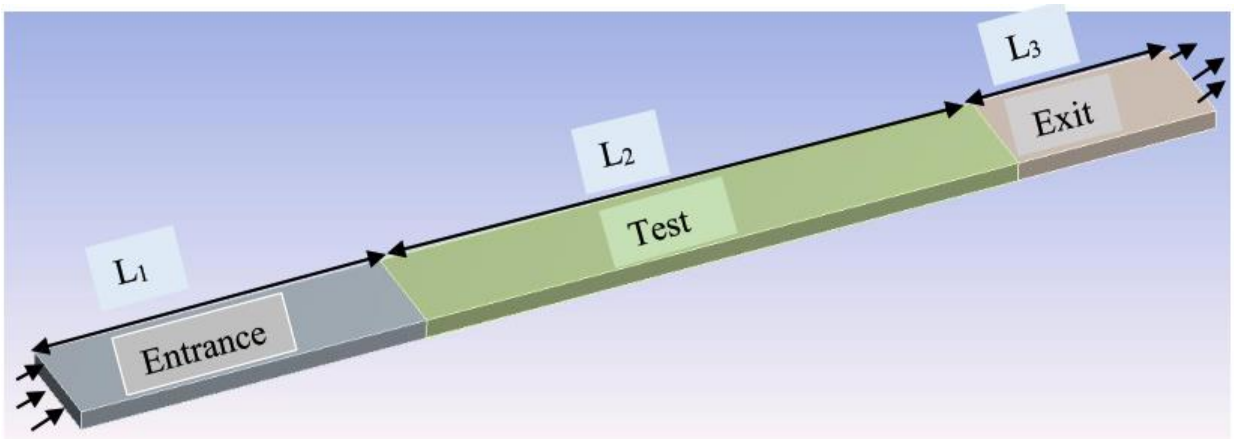

Figure 3.1: 3D Computational Image of SAH

According to ASHRAE Standard 93 [3], the minimum entrance length of the SAH duct is taken as L_1 = 5WH to ensure that the airflow becomes fully developed before entering the test section. Similarly, the minimum exit length is maintained as L_3 = 2.5WH, this arrangement ensures proper mixing of the heated air with the incoming airflow. The main geometrical constraints of SAH duct is considered in present work has been shown in table 3.1.

Table 3.1: Geometrical and operating parameters

Parameters	Value
Entrance length (L1)	350 mm
Test length (L2)	600 mm
Exit length (L3)	200 mm
Width (W)	100 mm
Height (H)	20 mm
Roughness pitch (P)	20 mm
Roughness height (e)	2 mm
Relative pitch (P/e)	10
Relative roughness width (W/w) – In Multi V+arc	6
Angle of attack (Ø) - In Multi V+arc	60^0
Aspect ratio of duct (W/H)	5
Constant insolation (I)	1000 W/m^2
Inlet velocity (u)	0.833 m/s^2 & 4.580 m/s^2
Reynolds number (Re)	3000 & 11000

To guarantee that the artificial roughness elements successfully disrupt the laminar sublayer that forms close to the absorber surface, the roughness height (e) is selected. According to the study [16], the roughness pitch (P) is chosen to enable appropriate flow separation and reattachment behind the ribs, which aids in enhancing heat transmission. In order to mimic turbulent flow

conditions commonly taken into consideration in solar air heater research, the airflow velocity is chosen to correspond to a Reynolds number range of 3000–11000. To replicate the average radiation of sun of clean sky, continuous heat flow of 1000 W/m² is applied on absorber plate. The above table provides a summary of the 3D solar air heater model's operational parameters.

In this study, two different geometrical configurations are examined: a V+arc shaped roughness and a multiple V+arc roughness arrangement. The following figures show how various designs perform in comparison to a smooth absorber plate.

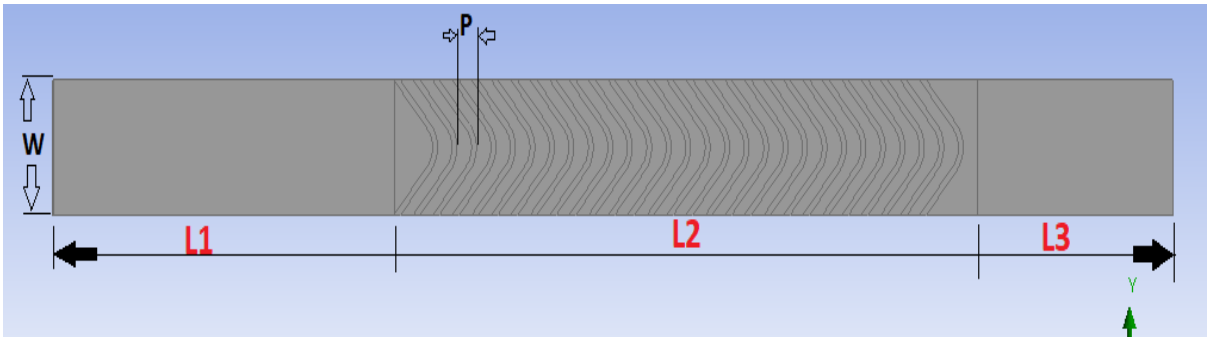

Figure 3.2: (a) Top view of V+arc shaped roughness geometry

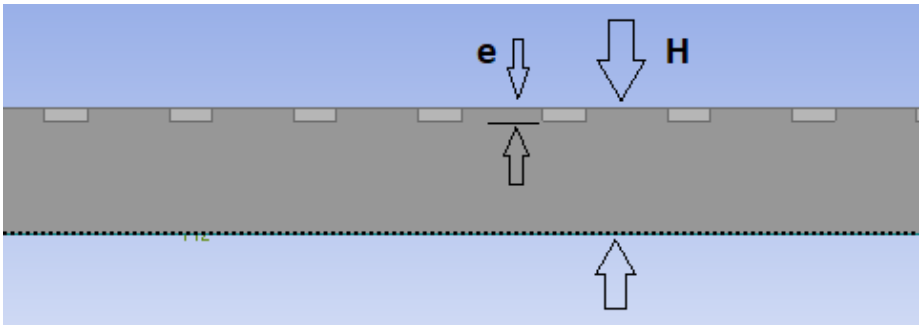

Figure 3.2: (b) Front view of V+arc shaped roughness geometry

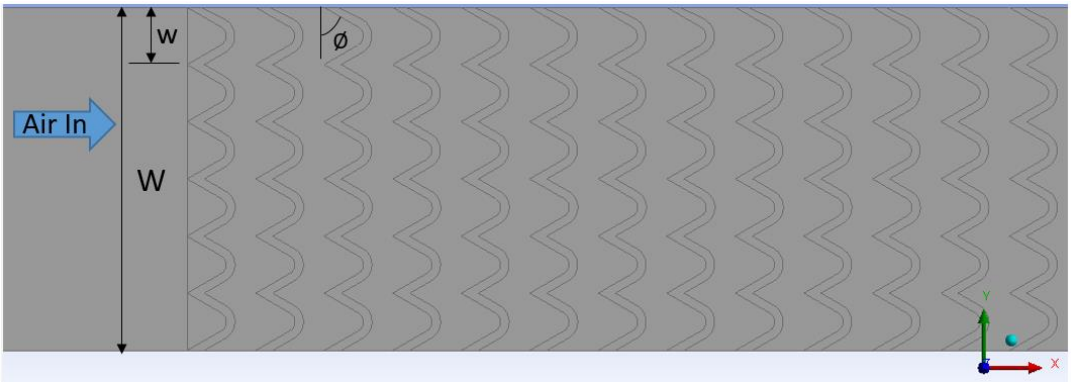

Figure 3.3: Multiple V+arc shaped roughness geometry

3.1.1. Turbulence model Selection

The numerical simulations assess a range of turbulence models, such as RNG k–ε, standard k–ε, standard k–ω, and SST k–ω, to determine which model is best for estimating the Nusselt number (Nu) in a smooth solar air heater duct. The results gained from these studies of models validated comparing to Dittus–Boelter correlation. A comparison of the predicted Nusselt numbers from the different turbulence models is presented in Figure 3.2.

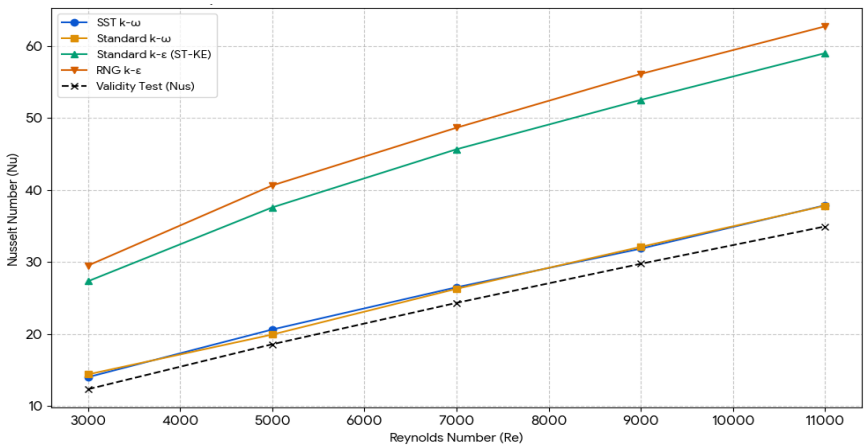

Figure 3.4: Nusselt no. prediction using various Turbulence model

It is detected from the comparison that the SST k–ω turbulence model provides the closest arrangement with the Dittus–Boelter correlation, with an average deviation of approximately 7.55%. Therefore, the SST k–ω model is adopted for the present investigation.

The key advantages of the SST k–ω model are that it combines the benefits of both the standard k–ε and standard k–ω turbulence models.

3.1.2. Governing equations

The governing equations, as described in the ANSYS Fluent 17.2 User's Guide [27], are applied to study heat transfer and the fluid flow behaviour in both smooth and roughened solar air heater (SAH) ducts.

- Continuity equation

$$\frac{\partial}{\partial x_j} u_j = 0 \qquad (1)$$

- Momentum equation

$$\frac{\partial(\rho u_i u_j)}{\partial x_j} = -\frac{\partial p}{\partial x_i} + \mu \frac{\partial}{\partial x_j}\left(\frac{\partial u_i}{\partial x_j} + \frac{\partial u_j}{\partial x_i}\right) + \frac{\partial(-\rho\overline{u_i' u_j'})}{\partial x_j} \quad (2)$$

- Energy equation

$$\frac{\partial(u_j T)}{\partial x_j} = \alpha \frac{\partial}{\partial x_j}\left(\frac{\partial T}{\partial x_j}\right) + \frac{\mu_t}{\rho \sigma_t}\frac{\partial}{\partial x_j}\left(\frac{\partial T}{\partial x_j}\right) \quad (3)$$

Where, u_i = velocity component in X direction

u_j = velocity component in Y direction

i, j = 1,2, and 3

3.1.3. Data reduction for CFD and experimental analysis

A 16-channel universal data recorder is used to record experimental data under steady-state circumstances, while CFD-Post is used to acquire the CFD results, which include air temperature, absorber plate temperature and pressure drop across the duct. The following formulae can be used to calculate how the V+arc configuration affects the Nusselt no. (Nu) and friction factor (f).

- Convective heat transfer coefficient (h): It is calculated with energy balance equation

$$Q = \dot{m} c_p (T_{out} - T_{in}) = h\, A_p\, (T_w - T_m) \quad (4)$$

- The average Nusselt number is defined as

$$Nu = \frac{h \times D_h}{k} \quad (5)$$

- Reynolds number is given below

$$Re = \frac{\rho u L}{\mu} \quad (6)$$

- Friction Factor is given below

$$f = \frac{2 \times \Delta P \times D_h}{L \times \rho \times u^2} \quad (7)$$

- The thermo hydraulic performance THP (denoted by η) is given below

$$\eta = \frac{(Nu_r/Nu_s)}{(f_r/f_s)^{\frac{1}{3}}} \quad (8)$$

- Dittus–Boelter equation is given below [2]

$$Nu_s = 0.023\, Re^{0.8} Pr^{0.4} \quad (9)$$

- Blasius equation for friction factor is given below [2]

$$f_s = 0.316\, Re^{-0.25} \quad (10)$$

3.1.4. Boundary condition

The Continuity, Momentum, and Energy equations are solved in CFD using the following boundary conditions. Other walls are regarded as insulated.

i. Inlet

- Air inlet Velocity (u) = 0.833 m/s & 4.580 m/s
- Air Inlet Temperature T_{in} = 300 K (atmospheric)
- Intensity of turbulence = 5%
- Hydraulic diameter (D_h) = 0.0333 m

ii. Absorber plate wall

- Constant insolation (I) = 1000 W/m^2 (uniform heat flux with no- slip condition)

3.1.5. Grid independence test

A structured hexahedral mesh is generated for the smooth duct, while a hybrid mesh is employed for the roughened configuration to accurately capture the complex rib geometry. Special attention is given to near-wall mesh refinement through the use of inflation layers.

A total of 10 inflation layers with growing rate of 1.5 are applied near all walls, and the first cell height is chosen to maintain $y^+ \approx 1$ throughout the test section. This ensures proper resolution of the viscous sub layer and accurate prediction of wall shear stress and heat flux.

Three meshes with ever finer resolution are used in a grid independence research. The average Nusselt number is used as the criterion to assess mesh sensitivity. The variation in Nusselt number between the medium and fine meshes is found to be less than 2%, indicating that further mesh refinement has a negligible effect on the solution.

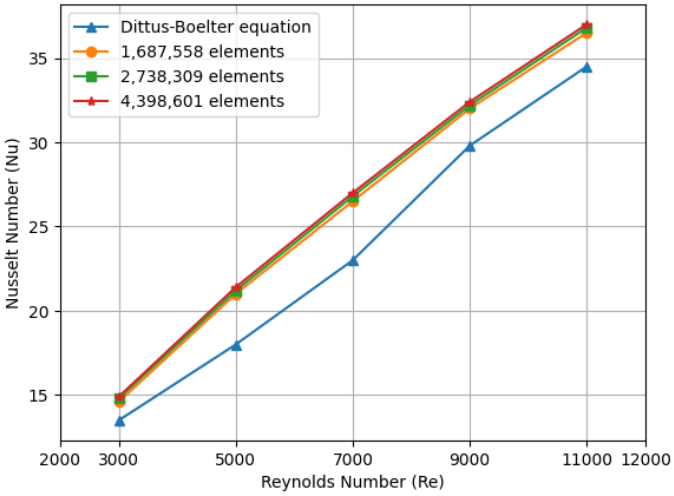

Figure 3.5: Grid independence study result for smooth absorber plate

Therefore, the medium mesh is chosen for all simulations as it offers a good compromise between numerical precision and computing expense. Furthermore, Figure 3.5 displays nearly equal values for meshes with 2.74 million and 4.40 million components, indicating that the solution has reached a stable, grid-independent state. The computational grid for the smooth, V+Arc, and multiple V+Arc geometries is illustrated in Figure 3.6.

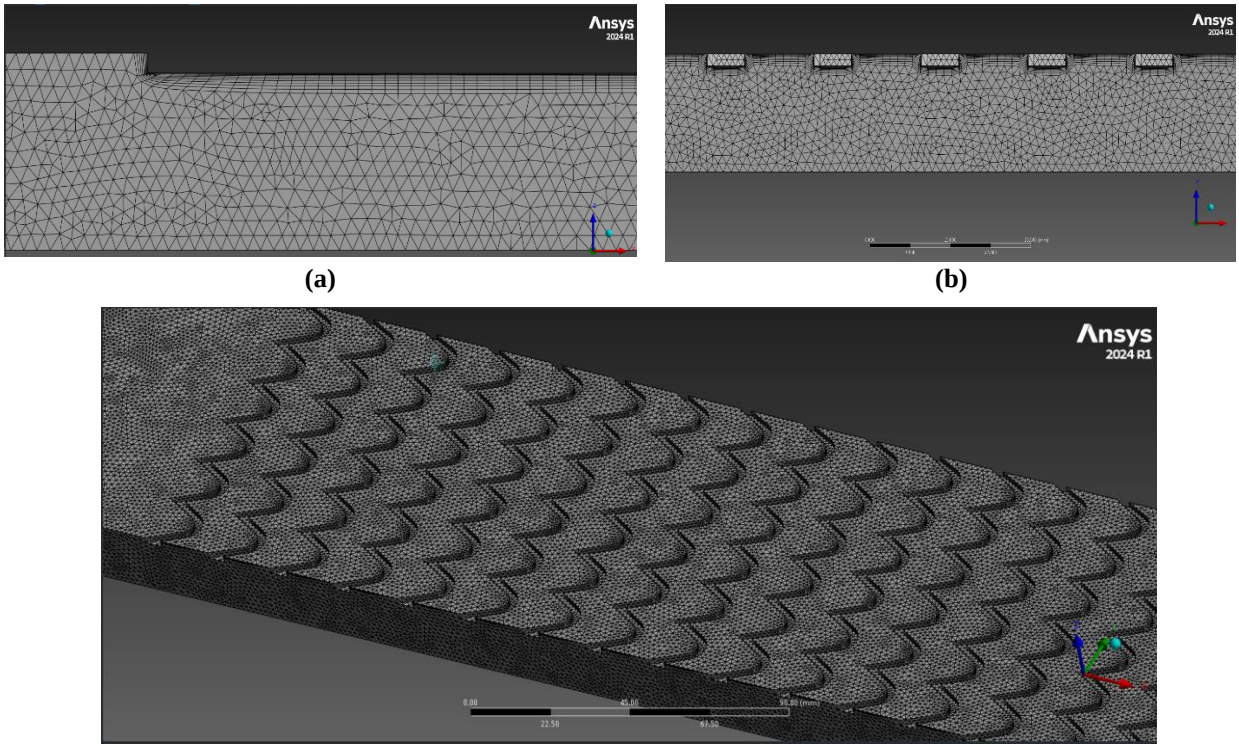

(a) **(b)**

(c)

Figure 3.6: Mesh generation for (a) Smooth surface (b) V+Arc Geometry (c) Multiple V+Arc Geometry

Chapter 4

Experimental Study

The design and construction of setup for experiment is created to examine the behaviour of heat transfer and airflow in SAH with artificial roughness on the absorber plate are shown in this chapter. In order to validate the theoretical conclusions, the system is built to collect trustworthy experimental data for heat transition, airflow characteristics, thermal efficiency, and THPP of SAH.

Experimental setup involves several components, including a rectangular wooden duct, a glass cover, electrical lamps used as the heat source, a differential manometer, a centrifugal blower, PT-100 temperature sensors (bolt type and probe type), a pyranometer, and a 16-channel universal data logger. A photographic view of the complete experimental arrangement is presented in Figure 4.1.

Figure 4.1: Experimental Set-up

The experiments are performed by adjusting the blower speed to achieve Reynolds numbers between 3000 and 11000. A uniform heat flux of 1000 W/m² is generated using electric lamps composed of twelve 100 W filament bulbs to replicate solar radiation conditions. A pyranometer has taken care to measure applied constant insolation's intensity. The necessary experimental data were recorded after the system reached quasi-steady-state conditions. Bolt-type thermal sensors were used to track the temperature of the absorber plate, while probe-type sensors were used to detect the air temperature. A differential manometer was used to measure the pressure decrease (ΔP) along the duct length. The tests were conducted at various Reynolds numbers on a smooth absorber plate. The following parameters were measured:

i. Absorber plate Temperature
ii. Air outlet Temperature
iii. Air velocity and Pressure drop (ΔP) in the duct

4.1. Smooth Absorber plate

Sample readings measured for smooth absorber plate is shown below for Re 5000

- **Absorber plate Temperature**: The temperature of absorber plate was monitored using nine PT-100 sensors, and the readings were documented at five different time intervals, as presented in Table 4.1.

Table 4.1: Sample readings for temperature on absorber plate

Time	Sensor 1 (°C)	Sensor 2 (°C)	Sensor 3 (°C)	Sensor 4 (°C)	Sensor 5 (°C)	Sensor 6 (°C)	Sensor 7 (°C)	Sensor 8 (°C)	Sensor 9 (°C)
0 min	72.7	73	73.4	73.6	73.8	74	73.9	74	73.7
2.5 min	73.6	73.9	74.2	74.4	74.7	74.8	74.8	74.8	74.6
5 min	74.3	74.6	74.9	75.2	75.5	75.7	75.6	75.7	75.4
7.5 min	74.8	75.1	75.5	75.8	76.1	76.2	76.2	76.2	75.9
10 min	75.2	75.5	75.9	76.2	76.5	76.6	76.5	76.6	76.2
Average	74.12	74.42	74.78	75.04	75.32	75.46	75.4	75.46	75.16
Average	75.01								

- **Air Temperature:** Temperature sensors are used for measuring air temperatures at the intake and outflow at five different time intervals.

Table 4.2: Sample readings for Air Inlet and outlet temperature

Time	Inlet Temperature (°C)	Outlet Temperature (°C)
0 min	25.0°C	32.0°C
2.5 min	25.1°C	31.0°C
5 min	25.3°C	32.1°C
7.5 min	25.3°C	31.5°C
10 min	25.4°C	32.2°C
Average	25.22°C	31.76°C

Air velocity and Pressure drop (ΔP) in the duct: Differential manometer has been used for measuring pressure drop.

Table 4.3: Sample readings for Air Inlet velocity and Pressure drop

Time	Air Velocity (m/s)	Pressure Drop (ΔP) (N/m^2)
0 min	2.27	5.43
2.5 min	1.91	4.6
5 min	1.91	4.6
7.5 min	2.15	5.01
10 min	2.15	4.81
Average	2.08	4.89

Chapter 5

Results and Discussion

This chapter examines the outcomes of different roughness geometries on heat transmission behaviour, fluid friction, and thermo-hydraulic performance. It also presents the three-dimensional (3D) simulation results together with the experimental findings for the smooth plate, V+Arc roughness, and Multiple V+Arc roughness configurations.

5.1. Effect on Nusselt number (Nu)

The impact of Reynolds Number (Re) on Nusselt Number (Nu) for three distinct Solar Air Heater (SAH) configurations Smooth Plate, V+Arc Geometry, and Multiple V+Arc Geometry is depicted in Figure 5.1.

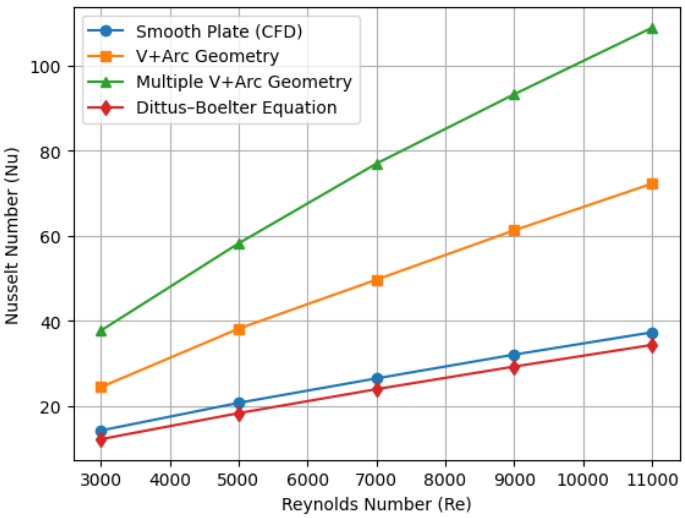

Figure 5.1: Nu Vs Re for different Roughness Geometries

1. **Direct Proportionality with Reynolds Number**: For all three tested geometries, the rise in Nusselt Number observed, for the Reynolds No. from 3000 to 11000. This happens as an outcome of greater turbulence and a thin thermal layer produced by higher flow velocities (higher Re), which promote more effective convective heat transfer.

2. **Superiority of Roughened Geometries:** Both artificial roughness configurations (V+Arc and Multiple V+arc) significantly outperform the smooth plate across the entire range of flow rates.
    - **Multiple V+Arc Geometry:** This configuration achieves the highest heat transfer enhancement, with Nu values rising from 37.67 at $e = 3000 to 108.93 at Re = 11000.
    - **V+Arc Geometry**: This configuration shows moderate improvement, with Nu values ranging from 24.38 to 72.25.
    - **Smooth Plate:** Serves as the baseline, recording the lowest heat transfer values, ranging from 14.17 to 37.27.
3. **Comparison with Standard Equations Validation of Experimental Data:** Nusselt No. for the smooth plate closely follows the Dittus-Boelter Equation.
    - **Enhancement Factor:** The Multiple V+Arc geometry provides an enhancement ratio approximately 2.9 to 3.1 times higher than the standard smooth plate baseline. This suggests that the multiple arc arrangement creates significant secondary flow and vortex generation, which disrupts the laminar sub-layer more effectively than a V+Arc or smooth surface.

5.2. Effect on Friction factor (f)

The impact of the Reynolds no. (Re) on the Friction Factor (f) for the various geometries is depicted in Figure 5.2 and is explored further:

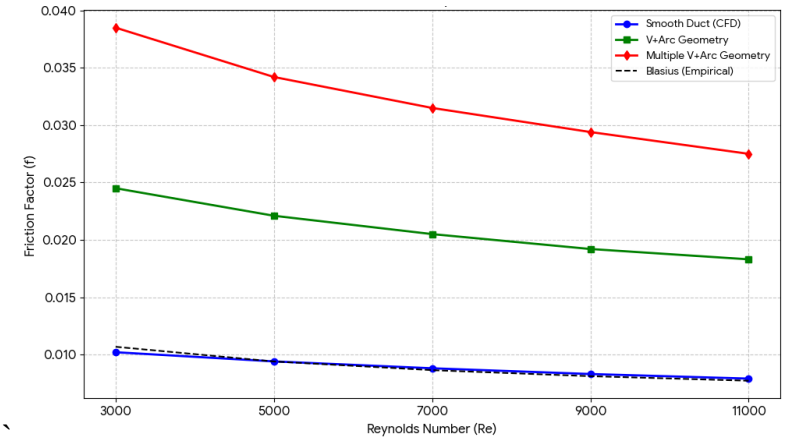

Figure 5.2: Friction factor Vs Re for different Roughness Geometries

1. **Inverse Relationship with Reynolds Number:** As the Reynolds Number increases from 3,000 to 11,000 for all three geometries, the friction factor falls. This trend occurs because the relative effect of viscous drag reduces as the flow becomes more turbulent at higher velocities.
2. **Roughness Penalty:** The introduction of artificial roughness significantly increases the flow resistance in comparison of the smooth duct baseline.
    - **Multiple V+arc Geometry**: This configuration exhibits the highest friction factor, ranging from approximately 0.030 to 0.027. The multiple arc arrangement creates intense flow separation and secondary vortices, which significantly increase the pressure drop.
    - **V+arc Geometry:** This geometry shows a moderate friction penalty, with values recorded between 0.017 and 0.015.
3. **Validation with Standard Equations:** The Blasius equation and the experimental results for the smooth duct correspond rather well. This strong correlation shows that the pressure drop data are trustworthy and validates the precision of the experimental equipment.
4. **Comparison of Magnitude:** For Reynolds number 3000, the friction factor for the Multiple V+Arc geometry is about 2.3 times greater than the smooth plate. Although this increase indicates a higher pumping power requirement, the overall system performance remains favourable because the improvement in heat transfer is comparatively larger.

5.3. Evaluation of Thermo hydraulic performance (THPP)

The THPP in figure 5.3 evaluates the overall effectiveness of the roughened solar air heater by comparing the relative increase in heat transfer to the relative increase in friction.

1. **Superiority of Multiple V+arc Geometry:** The Multiple V+arc configuration consistently demonstrates the highest performance across the entire range of Reynolds numbers (Re), with values ranging from 1.99 to 2.06.
2. **V+arc Performance:** The standard V+arc geometry shows moderate efficiency, with THPP values between 1.59 and 1.64. While this is a significant improvement over the smooth plate, it is approximately 20% less efficient than the Multiple V+arc design.
3. **Peak Performance Point:** For the Multiple V+Arc geometry, the maximum thermo-hydraulic performance parameter ($\eta = 2.06$) is obtained at $Re = 7000$. This indicates that,

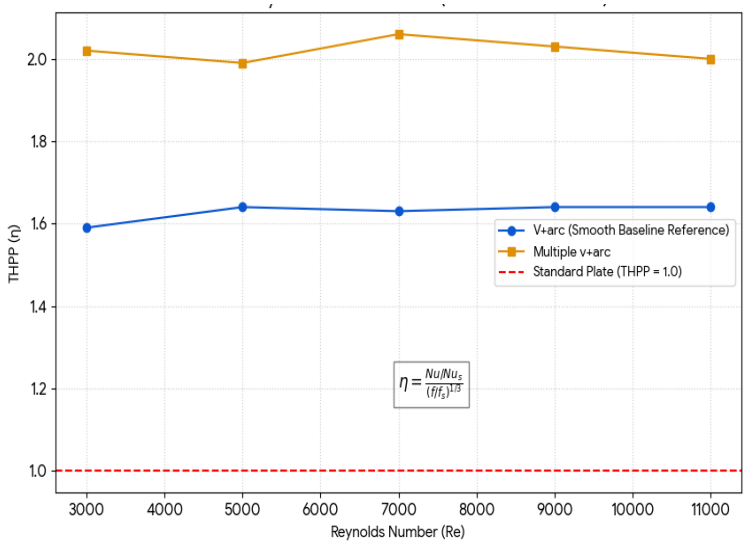

Figure 5.3: Evaluation of Thermo hydraulic performance parameter

at moderate flow conditions, an effective balance is achieved between heat transfer enhancement and the increase in friction losses.

5.4. Comparison of Experimental and CFD result for Smooth plate

The validation of the smooth plate baseline is a critical step to ensure the reliability of subsequent heat transfer enhancement measurements for the V+arc geometries.

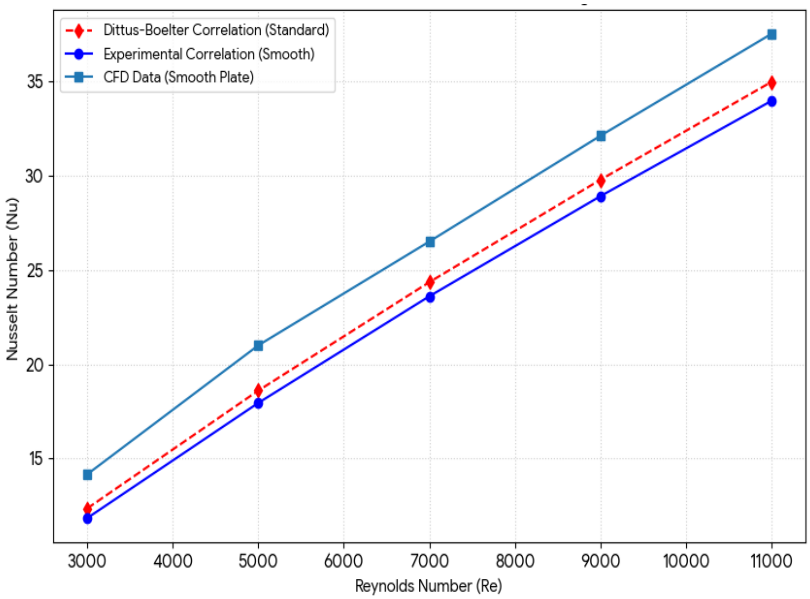

Figure 5.4: Experimental and CFD result for Smooth plate

1. **Experimental vs. CFD Results**: The CFD Data for the smooth plate shows a strong positive correlation with the experimental results. The CFD values, however, are

somewhat higher than the experimental ones, reaching around 37.5 at Re = 11000 as opposed to the experimental 33.95. The two lines' slopes are almost the same.

2. **Correlation Coefficient**: The close proximity and parallel nature of the Experimental and CFD lines indicate a high degree of correlation. This confirms that the numerical model effectively captures the physics of the turbulent flow regime within the Solar Air Heater (SAH) duct.

3. **System Accuracy:** The deviation between the experimental, CFD, and theoretical values remains within an acceptable engineering range (typically 10%). This small margin of error validates the accuracy of sensors, flow meters, and boundary conditions used for experimental test rig.

Chapter 6

Conclusions

The THPP of a solar air heater (SAH) with V+Arc and Multiple V+Arc artificial roughness geometries was investigated experimentally in present work. The following decisions are made in light of the data collected:

1. **Heat Transfer Enhancement:** Both roughened geometries significantly improved heat transfer compared to the smooth plate. The Multiple V+arc geometry achieved the highest Nusselt number Nu = 108.93 at a Reynolds number of 11,000, which is approximately 3.1 times greater than the standard smooth plate baseline.
2. **Friction Factor Penalty:** An increase in flow resistance was also linked to the improvement in heat transmission. The friction factor (f) for the Multiple V+Arc geometry varied between 0.030 and 0.027, indicating the highest pressure drop penalty among the tested configurations.
3. **Thermal Hydraulic Performance (THP):** For both geometries, the performance parameter (η) computation verified that the increases in heat transmission offset the friction losses. The Multiple V+arc geometry emerged as the most efficient design, maintaining a THPP value of approximately 2.0 across all tested flow regimes.
4. **Optimal Configuration:** The maximum thermal hydraulic performance η = 2.057 was observed for the Multiple V+arc geometry at Re = 7000. This indicates that the multiple V+arc arrangement is highly effective at disrupting the laminar sub-layer and promoting turbulence without an excessive pumping power requirement.
5. **Validation:** Experimental data for the smooth plate showed excellent agreement with the Dittus-Boelter and Blasius equations and computational data validating the reliability of the test facility and the reported results.

Publications

Sr. No.	Paper Title	Journal/Conference	Indexing
1.	Analysis of Heat Transfer Enhancement and Pressure Drop Characteristics in a Solar Air Heater Using V+Arc Shaped Artificial Roughness	Indian Journal of Natural Sciences. (IJONS) VOL-17/ISSUE 95/April 2026	WOS
2.	Comparative CFD Analysis of Heat Transfer and Flow Characteristics in a Solar Air Heater with Single and Multiple V+Arc Roughness	Journal of Applied Bio analysis, Vol. 11, No. 16s, December 2025 p. 83-93, (ISSN 2405-710X)	Scopus
3.	Artificial Roughness to enhance heat transfer characteristics of solar air heater — a comprehensive review	2nd International conference on emerging trends & contemporary practices (icetcp-2024) organized by Atmiya University, Rajkot	--

References

[1] J. G. Leishman, Introduction to Aerospace Flight Vehicles, Boundary Layer chapter. Daytona Beach, FL, USA: ERAU Press.

[2] J. A. Duffie and W. A. Beckman, Solar Engineering of Thermal Processes, 4th ed. Hoboken, NJ, USA: Wiley, 2013.

[3] ASHRAE Standard 93, "Method of Testing to Determine the Thermal Performance of Solar Collectors," American Society of Heating, Refrigerating and Air-Conditioning Engineers, Atlanta, GA, USA, 2003.

[4] A. E. Kabeel, M. H. Hamed, Z. M. Omara, and A. W. Kandeal, "Solar air heaters: Design configurations, improvement methods and applications – A detailed review," Renewable and Sustainable Energy Reviews, vol. 70, pp. 1189–1206, 2017.

[5] A. Singh Yadav and M. K. Thapak, "Artificially roughened solar air heater: Experimental investigations," Renewable and Sustainable Energy Reviews, vol. 36, pp. 370–411, 2014.

[6] V. S. Hans, R. P. Saini, and J. S. Saini, "Performance of artificially roughened solar air heaters – A review," Renewable and Sustainable Energy Reviews, vol. 13, pp. 1854–1869, 2009

[7] J. Nikuradse, "Laws of flow in rough pipes," Journal of Applied Physics, vol. 3, p. 399, 1950.

[8] D. F. Dipprey and R. H. Sabersky, "Heat and momentum transfer in smooth and rough tubes at various Prandtl numbers," International Journal of Heat and Mass Transfer, vol. 6, pp. 329–353, 1963.

[9] I. Singh and S. Singh, "A review of artificial roughness geometries employed in solar air heaters," Renewable and Sustainable Energy Reviews, vol. 92, pp. 405–425, 2018

[10] Varun, R. P. Saini, and S. K. Singal, "A review on roughness geometry used in solar air heaters," Solar Energy, vol. 81, pp. 1340–1350, 2007

[11] M. J. Lewis, "Optimising the thermohydraulic performance of rough surfaces," International Journal of Heat and Mass Transfer, vol. 18, pp. 1243–1248, 1975.

[12] V. S. Hans, R. P. Saini, and J. S. Saini, "Heat transfer and friction factor correlations for a solar air heater duct roughened artificially with multiple V-ribs," Solar Energy, vol. 84, pp. 898–911, 2010.

[13] J. S. Saini, "Effect of artificial roughness on heat transfer and friction factor in solar air heater," Solar Energy, vol. 41, pp. 555–560, 1988.

[14] T. Alam and M. H. Kim, “A critical review on artificial roughness provided in rectangular solar air heater duct,” Renewable and Sustainable Energy Reviews, vol. 69, pp. 387–400, 2017.

[15] D. Gupta, S. C. Solanki, and J. S. Saini, “Heat and fluid flow in rectangular solar air heater ducts having transverse rib roughness on absorber plates,” Solar Energy, vol. 51, no. 1, pp. 31–37, 1993.

[16] S. K. Verma and B. N. Prasad, “Investigation for the optimal thermohydraulic performance of artificially roughened solar air heaters,” Renewable Energy, vol. 20, no. 1, pp. 19–36, 2000.

[17] M. M. Sahu and J. L. Bhagoria, “Augmentation of heat transfer coefficient by using 90° broken transverse ribs on absorber plate of solar air heater,” Renewable Energy, vol. 30, no. 13, pp. 2057–2073, 2005.

[18] R. P. Saini and J. S. Saini, “Heat transfer and friction factor correlations for artificially roughened ducts with expanded metal mesh as roughened element,” International Journal of Heat and Mass Transfer, vol. 40, no. 4, pp. 973–986, 1997.

[19] J. L. Bhagoria, J. S. Saini, and S. C. Solanki, “Heat transfer coefficient and friction factor correlations for rectangular solar air heater duct having transverse wedge shaped rib roughness on the absorber plate,” Renewable Energy, vol. 25, no. 3, pp. 341–369, 2002.

[20] A. M. E. Momin, J. S. Saini, and S. C. Solanki, “Heat transfer and friction in solar air heater duct with V-shaped rib roughness on absorber plate,” International Journal of Heat and Mass Transfer, vol. 45, no. 16, pp. 3383–3396, 2002.

[21] S. Hans, R. P. Saini, and J. S. Saini, “Heat transfer and friction factor correlations for a solar air heater duct roughened artificially with multiple V-ribs,” Solar Energy, vol. 84, no. 6, pp. 898–911, 2010.

[22] A. Kumar, R. P. Saini, and J. S. Saini, “Development of correlations for Nusselt number and friction factor for solar air heater with roughened duct having multi V-shaped with gap rib as artificial roughness,” Renewable Energy, vol. 58, pp. 151–163, 2013.

[23] K. Nidhul, S. Kumar, A. K. Yadav, and S. Anish, “Computational and experimental studies on the development of an energy-efficient drier using ribbed triangular duct solar air heater,” Solar Energy, vol. 209, pp. 454–469, 2020.

[24] I. Singh, S. Vardhan, S. Singh, and A. Singh, “Experimental and CFD analysis of solar air heater duct roughened with multiple broken transverse ribs: A comparative study,” Solar Energy, vol. 188, pp. 519–532, 2019.

[25] K. Kumar, D. R. Prajapati, and S. Samir, “Heat transfer and friction factor correlations development for solar air heater duct artificially roughened with S-shape ribs,” Experimental Thermal and Fluid Science, vol. 82, pp. 249–260, 2017.

[26] Afshari, A. Sözen, A. Khanlari, A. D. Tuncer, and C. Şirin, “Effect of turbulator modifications on the thermal performance of cost-effective alternative solar air heater,” Renewable Energy, vol. 158, pp. 297–310, 2020.